

COST/PERFORMANCE TRADEOFFS FOR REFLECTORS USED IN SOLAR CONCENTRATING DISH SYSTEMS

Charles E. Andraka

Sandia National Laboratories
Albuquerque, NM 87185, USA

ABSTRACT

Concentrating Solar Power (CSP) dish systems use a parabolic dish to concentrate sunlight, providing heat for a thermodynamic cycle to generate shaft power and ultimately, electricity. Currently, leading contenders use a Stirling cycle engine with a heat absorber surface at about 800°C. The concentrated light passes through an aperture, which controls the thermal losses of the receiver system. Similar systems may use the concentrated light to heat a thermochemical process.

The concentrator system, typically steel and glass, provides a source of fuel over the service life of the system, but this source of fuel manifests as a capital cost up front. Therefore, it is imperative that the cost of the reflector assembly is minimized. However, dish systems typically concentrate light to a peak of as much as 13,000 suns, with an average geometric concentration ratio of over 3000 suns.

Several recent dish-Stirling systems have incorporated reflector facets with a normally-distributed surface slope error (local distributed waviness) of 0.8 mrad RMS (1-sigma error). As systems move toward commercialization, the cost of these highly accurate facets must be assessed. However, when considering lower-cost options, any decrease in the performance of the facets must be considered in the evaluation of such facets.

In this paper, I investigate the impact of randomly-distributed slope errors on the performance, and therefore the value, of a typical dish-Stirling system. There are many potential sources of error in a concentrating system. When considering facet options, the surface waviness, characterized as a normally-distributed slope error, has the greatest impact on the aperture size and therefore the thermal losses. I develop an optical model and a thermal model for the performance of a baseline system. I then analyze the impact on system performance for a range of mirror quality, and evaluate the impact of such performance changes on the economic value of the system. This approach can be used to guide the evaluation of low-cost facets that differ in performance and cost. The methodology and results are applicable to other point- and line-focus thermal systems including dish-Brayton, dish-Thermochemical, tower systems, and troughs.

INTRODUCTION

Concentrating Solar Power systems use parabolic reflectors, or approximations thereof, to concentrate sunlight. The concentrated energy is then absorbed as heat which is used to drive a thermodynamic or thermochemical cycle. Dish Stirling systems have demonstrated the highest net solar conversion efficiency, with the Stirling Energy Systems (SES) recent world record of 31.25% net conversion to grid-read electricity [1]. The dish-Stirling system attains its high efficiency through high concentration ratios, allowing the thermal losses to be decoupled from the absorber design through the use of a loss-limiting aperture. This high concentration ratio requires a high level of system optical efficiency.

In order to generate electricity at feasible cost, the system capital cost must be minimized. This is particularly important in utility-scale deployments, such as those planned by SES [2], where the revenue is on the utility side of the meter. The Department of Energy (DOE) goals for the Levelized Energy Cost (LEC) for dish-Stirling systems is \$0.06/(kW-hr) [3]. In order to reach this goal, SES has determined a need for total system installed cost at \$2/W, or \$50000 for a 25 kW rated system [4]. These goals require cost reduction associated with every part of the system. So far, dish-Stirling systems have been individual units hand-made by expert engineers, with corresponding prototype-level costs. However, loss in system performance caused by the decreased performance of a lower cost component may completely offset the intended system cost reduction. It is the purpose of this paper to highlight the tradeoff between cost of the reflective facets and the optical quality of these facets, so that reasonable economic decisions can be made for the collector component.

A number of optical deviations from perfection can impact the performance and durability of dish-Stirling systems. Table 1 highlights some of the recognized sources of optical error, and their potential impact on the system. There are two primary impacts of optical imperfections, service life and performance reductions. Error sources that simply impact the aperture size will reduce performance. However, errors that can increase the peak flux on the receiver will impact the receiver's service lifetime. It is also important to recognize the difference between random and systematic errors. Randomly-distributed errors can generally be characterized as an RMS (root-

TABLE 1. ERROR SOURCES, IMPACTS, AND MITIGATION TECHNIQUES FOR MODERN DISH SYSTEMS.

Error Source	Manifestation	Impact of Error	Mitigation Approach
Small scale facet slope error (random and distributed)	Aperture size Sidewall heating	Performance Performance	Subject of paper
Facet shape error (systematic shape errors)	High Peak flux Aperture size	Service Life Performance	Mirror manufacturing techniques
Structural deflections (systematic pointing errors)	High Peak Flux Aperture size	Service Life Performance	Modern analytical design tools minimize weight while improving stiffness
Facet alignment errors (random)	Aperture size Peak flux if large facets	Performance Service Life	Modern alignment techniques minimize this issue. In particular, automate image interpretation.
Facet alignment errors (systematic, due to operator or method errors)	Peak flux	Service Life	Validate tools and methods
Tracking (backlash, installation imperfections)	Aperture size Un-centered image	Performance Performance	Closed loop tracking

mean-squared) error, which is the standard deviation of the slope error of the collector surface and implies a normally-distributed error. Systematic errors generally cannot be characterized in the same way, and can lead to “flux pile-up” issues that are not predicted with a normal distribution approximation. Systematic errors may include facet shape errors, alignment errors, structural deflections due to gravity and wind, and tracking system errors. Through experience with the Sandia National Laboratories Advanced Dish Development System (ADDS) [5,6], we also recognize that most of these impacts can be minimized through careful design, manufacturing quality control, quality alignment tools, and closed-loop tracking controls. From this experience and indications from prior studies [7], we find that the size of the aperture has a very strong impact on system performance. In the case of the present study, we desire to optimize the aperture size as driven by the facet accuracy, and then compare the impact of this aperture size on system performance and economic viability.

Reflective facet accuracy, in recent years, has been consistently determined through the use of the Sandia/National Renewable Energy Laboratory (NREL)-developed V-SHOT (Video Scanning Hartmann Optical Tester) system [8]. This system measures the actual slope error at a large number of points across the mirror facet, and compares this measured slope to the “ideal.” The definition of “ideal” has not been consistent through the development of the V-SHOT tool. In some cases, the ideal is a true parabolic shape, in some cases the design shape of the particular facet technology, and in some cases a “best fit” polynomial or other curve. It is important when comparing technologies to attempt to compare them on a consistent basis. For this report, the key point is that the many “commercial” facet designs that have been characterized tend to have fairly high slope error values compared to the “structural” facets demonstrated on the ADDS and later incorporated by SES.

We are interested in a slope error that can be characterized by a normally-distributed localized random error across the facet surface. This imperfection will spread the reflected/focused sunlight in a conical fashion as it approaches the receiver. Large-scale, or systematic errors, may or may not be limitations of the manufacturing process, but are not well-modeled by the random error approximation. The figure of merit for random errors is the “RMS” slope error, which is the 1-sigma characterization of the error distribution. This is typically reported for the two principle axes separately, but many manufacturing methods produce a facet with similar errors in both axes. In addition to the spreading through random slope errors, the focused light is spread by deviations from a perfect parabola. For example, a number of dishes (Test Bed Concentrators [9], Advanco [10], SES) approximate a parabola through the use of spherical-contour facets. Given enough facets, the dish is a “piecewise

spherical” parabola, very similar to drawing a “piecewise linear” simulation of a circle with small straight line segments. The more segments that are used, the more the joined lines begin to look like a circle. Such deviations from a true parabola may be distributed sufficiently to be characterized by the normally-distributed random error approximation.

MIRROR FACET OPTICAL ERRORS

In this section I will review the reported facet slope errors for a range of prototype systems developed over the last few decades. This gives a frame of reference for what has been viewed as possible for commercial scale concentrator facets. Table 2 summarizes the slope errors reviewed in this section.

Laboratory dish systems such as Sandia’s Test Bed Concentrator (TBC) have expensive but highly accurate facets. The TBC facets were measured at a nominal 0.5 mrad slope error [11]. A foam-glass substrate supports a thin glass and silver reflective surface and provides the design curvature. The foam glass is hand ground to the correct shape on a mandrel, which is an expensive process. The facets are spherical in contour. The prototype Advanco Vanguard system has 336 spherical-contour facets that are also reported to be 0.5 mrad slope error [11].

During the late 1980s and early 1990s, several attempts were made to use stretched membrane concentrator facets. In this concept, a thin membrane is supported by a lightweight structural ring, and a slight vacuum behind the membrane provides a near-spherical shape. Cummins Power Generation used 24 1.524m diameter facets with an aluminized Mylar film as the reflective surface [11]. While this Compendium [11] reports a slope error of 1.5 mrad, other more detailed reports [12] indicate a range of slope errors from 1.5 to 2.5 mrad. Science Applications International Corporation (SAIC) and Solar Kinetics Inc. (SKI) used stainless steel stretched membranes on a 3.0 m facet [11], with a reported slope error range of 1.2 to 3.5 mrad. However, SAIC further reports [13] that they never achieved better than 2.5 mrad with the stretched membrane approach. On a larger scale, several companies have attempted single-facet stretched membrane dish systems. One notable example is the Distal II systems in Spain, built by Schlaich, Bergermann und Partner GbR (SBP). These systems had a slope error of just over 3 mrad compared to an ideal parabola, but less than 1.5 mrad when compared to a best-fit 10th-order polynomial [14]. This demonstrates the difficulty of separating local errors (random) from dish-scale errors (systematic) when considering large-facet systems.

SAIC built a prototype system with each facet made from many smaller flat, square subfacets [13]. They built two versions, one with

0.3m square subfacets for Concentrating Photovoltaics (CPV), and one with 0.15m square subfacets for dish-Stirling systems. They report slope errors of 2 mrad, but this was as compared to ideal flat multiple subfacets, not compared to the parabolic contour. Therefore, this was simply a characterization of the accuracy of mounting each subfacet at a particular angle. If one assumes the desired profile is spherical, the error due to the flat subfacet can be determined by integrating the slope of a spherical element across the area of the flat subfacet. If a radius of curvature of 16.25m is assumed (one of the radii of the McDonnell Douglas (MDAC) 25-kW system [15, 16]), the 0.15m flat subfacets would have an effective RMS slope error of 3.8 mrad, assuming they were placed perfectly and had no local imperfections. The total system effective slope error compared to a parabola would then be over 4 mrad.

A commonly considered facet approach for dish concentrators is the thick slumped glass similar to that used by trough systems. In this approach, the glass provides the facet structure as well as the reflective surface. The glass is thermally formed to a spherical or parabolic shape. Few dishes have been built this way, but a large number of trough systems use this mirror approach. The baseline Solargenix 1st-generation trough was measured at 4.4 mrad accuracy, but this included a small amount of mis-alignment of the panels. A next-generation Solargenix module was measured “approaching 3.0 mrad” by NREL [17]. This measurement also included alignment errors, since an entire trough section was characterized. Estimates indicate that the local imperfections might be less than 2.0 mrad slope error. No results could be found for dishes incorporating slumped glass.

MDAC developed a 25 kW system with a stamped steel facet and a thin glass reflective surface. This system is reported to have a slope error of 0.6 mrad [15]. However, more recent measurements by the NREL V-SHOT system indicate a slope error of 1.5 mrad [18]. The dish uses 82 spherical contour facets with 5 different radii of curvature to simulate a parabola. The stamped steel facets showed great promise in accuracy and potential cost, but the cost of prototype stamping dies is high. In production, this approach is seen as very viable [19]. Acurex incorporated a stamped steel construction into a single-facet 15 m dish [11], with a goal slope error of 2-3 mrad. However, the dish was damaged in high winds before measurements could be completed.

Several companies have demonstrated facets built on mandrels

TABLE 2. PROTOTYPE FACET SLOPE ERRORS.

Company	Facet Construction	Slope Error (mrad)
Sandia TBC	Foam Glass	0.5
Advanco	Foam Glass	0.5
Cummins	Mylaer stretched membrane	1.5 - 2.5
SAIC	Stainless stretched membrane, facets	2.5 - 3.5
SKI	Stainless stretched membrane, whole dish	1.2 - 3.5
SAIC	Flat subfacets	4+
Solargenix	Slumped thick glass, trough	2.0 - 4.0
MDAC	Stamped steel with thin glass	0.6 - 1.5
Acurex	Single facet stamped steel	2.0 - 3.0 goal
Paneltec/ Sandia	ADDS sandwich aluminum facets, thin glass	0.8 - 1.4
Sandia TBC	Sandwich construction replacement mirrors	0.4 - 1.0
SES/Paneltec	Sandwich construction, thin glass	0.8

with various fiberglass lay-ups. However, no detailed public information on slope error characterization is available.

Sandia National Laboratories and Paneltec developed a sandwich-construction structural facet [20]. This construction was first implemented on the ADDS, and had a reported accuracy of 0.8 to 1.4 mrad [21]. The ADDS facets were somewhat larger than the original structural facet prototypes developed for Sandia’s TBC. These original attempts at structural facets demonstrated a slope error of 0.4 to 1.0 mrad [20]. In 1998 the material cost for prototype facets estimated at \$56.38/m² [20], and production material cost was estimated at under \$36/m². The cost of materials has risen, and we do not have current estimates on the cost potential in production. The 1998 cost estimates for the structural facets are for materials only, and it is assumed that in production the labor content could be reduced to very little. These cost estimates were seen as very competitive with poorer-performing low-cost facets at the time. This construction has more recently been incorporated on the SES prototype systems [22], which are patterned after the MDAC systems. SES reduced the part count to two radii of curvature after determining that the outermost mirrors effectively determine the system aperture size. We will use published data on this SES system as a baseline design for our mirror performance analysis.

DEFINITION OF BASELINE SYSTEM

The SES system incorporates a Mark II Kockums 25kW Stirling engine, which was also used on the Advanco and MDAC systems. The Paneltec structural sandwich facets have been measured by NREL’s V-SHOT system at approximately 0.8 mrad RMS slope error. Sandia National Laboratories developed an improved alignment strategy that smoothes the flux pattern on the receiver, filling in the gap from the support pedestal, without compromising the aperture size [23]. The radii of curvature selection has been reduced to two sizes, compared to the 5 used on the MDAC system [22]. A 0.19 m diameter aperture is used to control re-radiation and reflection losses from the receiver cavity [23].

The total dish area is 87.7m² of solar intercept area [11]. The system performance at steady state conditions is very linear with insolation (Figure 1) [24], as expected for dish-Stirling systems [25]. The deviations from a straight line at 600 W/m² are caused by the startup thermal transient. Similarly, the drop in output at 1000 W/m² is during a short dense cloud transient. A nominal performance curve can approximate the system performance, as shown in Figure 1. This line passes through 25 kW net rated power at 1000 W/m², and zero output power at about 200 W/m² insolation. This idealized performance will be used in the analysis. The cost of this system in large installations is expected to be \$2/W or better [4]. We will use this estimate when looking at the economic impacts of facet quality.

The receiver cavity consists of the absorber tube bundle, surrounded by a cylindrical ceramic cavity, a conical entry cone that supports the aperture, and a ceramic center plug that protects the top of the engine [11]. Figure 2 shows a published cross section of the receiver cavity, along with the idealization used to model the cavity performance. Note that later versions of the MDAC receiver design on the Kockums engine included the conical sidewall for the lower portion, as modeled. The center plug on the actual receiver is re-entrant (sticks back into the cavity), which cannot be modeled easily with existing tools. However, a detailed analysis indicates that simulating this protective plug with a flat plate of ceramic is a reasonable approximation, with a difference in predicted thermal losses of less than 20 W.

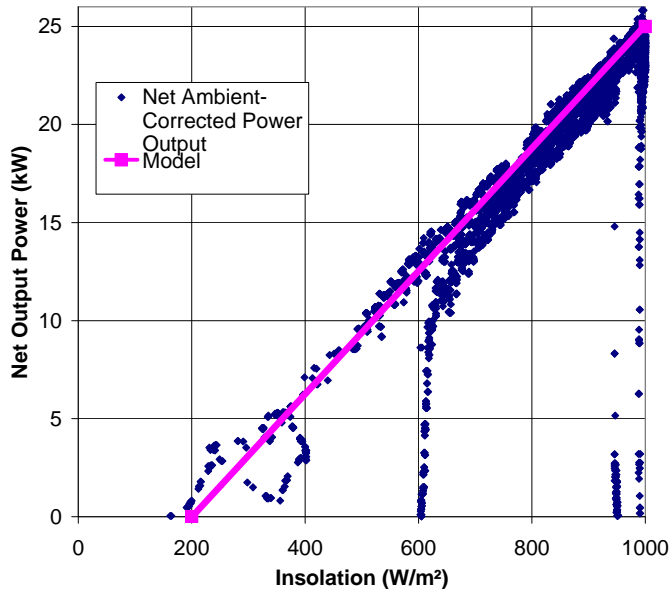


Figure 1. System net power performance curve, showing the nominal performance model curve and actual data. The deviations at 600 W/m² and 1000 W/m² are caused by transient thermal effects during startup and a cloud transient.

OPTICAL AND THERMAL MODELS

The reflective optics of the system were modeled with Sandia's CIRCE2 dish modeling program [26]. This well-known model convolves the sun shape with the normally-distributed slope error of the facets to generate an incident solar flux on an axis-symmetric receiver cavity of arbitrary shape. For most of the analysis, I assume a nominal 1000 W/m² insolation on the dish and 94% reflectivity. I assume perfect tracking and alignment, with the only imperfection being the facet slope error. The baseline system CIRCE2 model

predicts 82.5 kW incident into the receiver cavity through the 0.190 m aperture, with 69.0 kW directly incident on the absorber tubes. For most of the models, unless noted, the receiver cavity shape and position were not changed. The 82 mirror positions were based on the MDAC mirror layout, and the mirrors were 1.22 m x 0.91 m each. The Sandia-developed alignment strategy [23] was implemented for all cases. Figure 3 shows the baseline incident flux pattern on the engine absorber tubes [23] as predicted by CIRCE2.

Sandia National Laboratories AEETES [27] thermal cavity modeling code was used to evaluate the net thermal transport within the cavity and predict the total energy losses and absorbed energy, based on the CIRCE2-predicted incident fluxes. AEETES is a 2-D model that accounts for the solar-band diffuse reflections in the cavity to develop a net solar input flux on each element, and then accounts for thermal radiation, conduction, and convection to develop a temperature field and net flux in the entire cavity. From this, the thermal losses and net absorbed power can be determined. The convection is based on the Stine correlation [28] at 45 degrees dish elevation. Conduction is limited to 1-D radial or axial conduction. I assumed 0.05m of insulation on the cylindrical sidewall, and 0.15m on the conical sidewall and the center plug. The insulation conductivity was set to 0.5 W/m·K, with convection on the outside at 40 W/m²·°K to 293 °K air. The absorber face temperature was set to 800 °C, which is consistent with a working fluid operating temperature of 720 °C at the anticipated flux levels. All of the ceramic had a solar-band absorptivity of 20% (reflectivity 80%), and a thermal-band emissivity of 80%. The absorber tubes had a solar band absorptivity of 89% and an emissivity of 85%, as is typical in analyzing such receivers with Inconel surfaces. The results may be sensitive to these properties, but they were held constant for the purposes of this study. A detailed study of the sensitivity to these properties is presented by Diver [7].

ANALYSIS AND RESULTS

A matrix of runs was developed in which the normally-distributed slope error was varied over the range of 0.8 mrad to 3.5 mrad, covering the baseline case and most of the published potential facet qualities. At each modeled slope error, the aperture size was varied from 15.24 cm to 35.5 cm in diameter (6 in to 14 in). When the

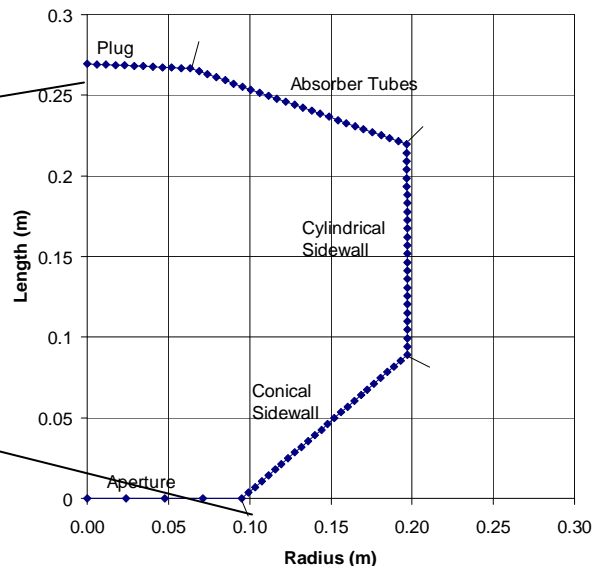
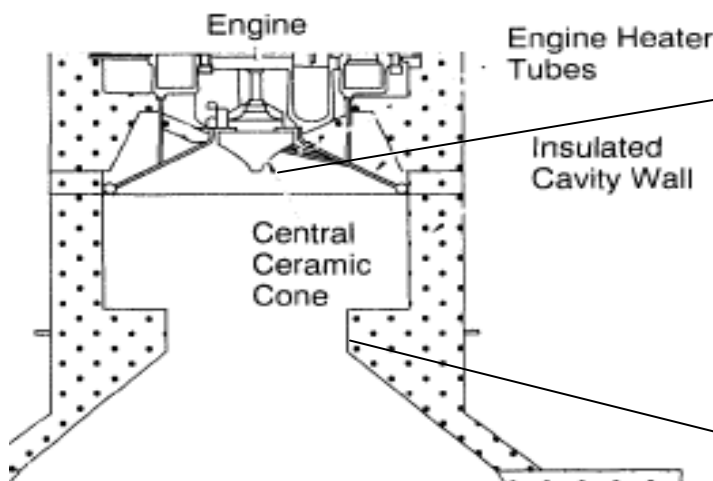


Figure 2. Receiver cavity and model. The conical sidewall is a later addition after the published drawing. The center plug is modeled as a flat plate to accommodate model limitations.

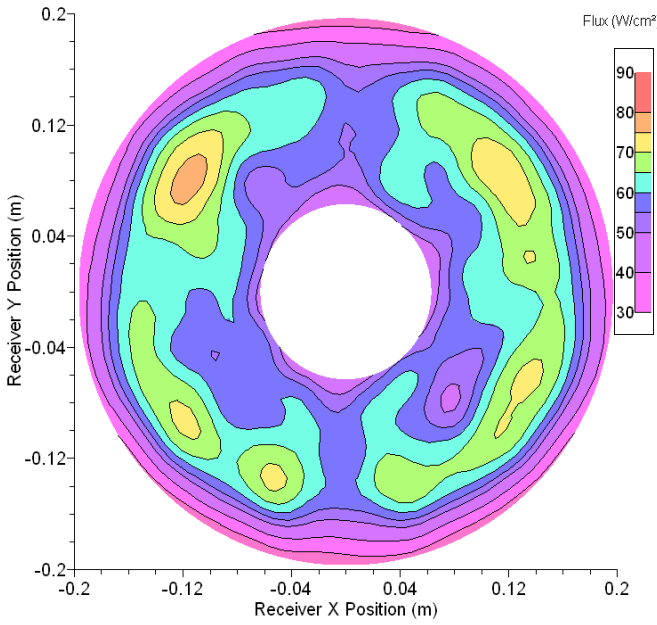


Figure 3. Flux distribution on absorber tube array as predicted by CIRCE2, using the Aperture Restrained dynamic alignment strategy [23]

aperture is too small, significant concentrated light is intercepted by the edges of the aperture and never makes it to the receiver (intercept losses). When the aperture gets larger, the thermal losses increase. The net result is that an optimum can be determined for each slope error. As the slope error gets larger, the image size at the aperture is larger, and the aperture must be larger to prevent spillage. Figure 4 shows the net power absorbed by the engine tubes in each case, with a clear optimum in aperture size for each facet slope error. The baseline case of 0.8 mrad slope error has an optimum at 17.8 cm diameter (7.0 in), whereas we have experimentally determined that the optimum is

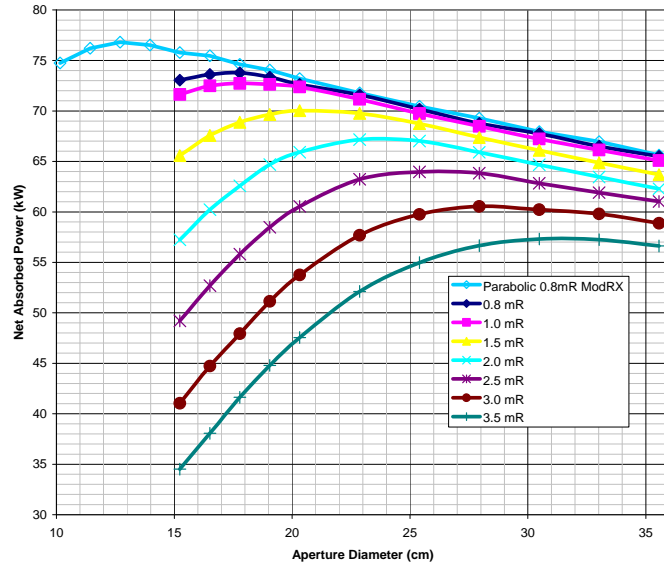


Figure 4. Absorbed power as predicted by CIRCE2 and AEETES for a range of slope errors and aperture sizes. Note the clear optimum aperture size for each slope error.

between 17.8 and 19.0 cm (7.0 and 7.5 in). This means that the remainder of the errors that impact aperture size such as structural deflections, alignment errors, and tracking errors are very well controlled on this system, and are virtually negligible.

Figure 5 shows the loss components for the optimum cases at each slope error. Notice that the conduction and convection change little, but the reflection, re-radiation, and intercept terms increase dramatically with the increased slope error. However the re-radiation does not increase with T^4 as expected. This is for several reasons. First, as the aperture is opened, there is less cavity effect. The effective absorptivity approaches the absorptivity of the heated surface materials. Second, more of the light is incident on the white sidewalls, which have a lower absorptivity than the tubes.

Since the higher slope error models put more flux on the sidewalls and less on the tubes directly, the peak flux on the tubes is decreased. I ran one case at 3.0 mrad in which I moved the absorber tube bundle 0.0254 m closer to the aperture so that the peak flux returned to near nominal levels. However, the losses were only minimally reduced compared to those associated with the baseline receiver cavity size/shape. While the losses due to reflection from the sidewalls was reduced by moving the absorber toward the aperture, the view factor from the absorber to the aperture was increased, and so reflection and re-radiation from the absorber increased as well.

Recognizing that the SES dish is a simulation of a parabola, it is also instructive to determine the loss of performance due to this compromise of a true parabola. While a physical dish would have compromises for structural support, blockage, etc., I modeled the ideal dish as a continuous parabola. I did insert a hole in the center of the parabola, since the engine package will cause a shadow. For simplicity in this model, I varied the hole size until the power on the center plug matched that of the baseline case. I then adjusted the outer diameter until the total intercept area of the dish matched the baseline case as well. The focal length/diameter ratio (f/d) of the round dish was held at 0.6. This resulted in a 10.9 m diameter dish with a 2.5 m diameter hole, and a focal length of 6.528 m. The absorber was positioned to provide the same spillage onto the outer cylindrical sidewall as the baseline case, which resulted in moving the absorber .0254 m closer to the aperture. The result is also shown in Figure 4, where the optimum is seen at a 12.7 cm diameter aperture, and an additional 3 kW thermal energy is absorbed into the engine. This demonstrates the extent of the compromise of the parabolic shape due to the piecewise-spherical

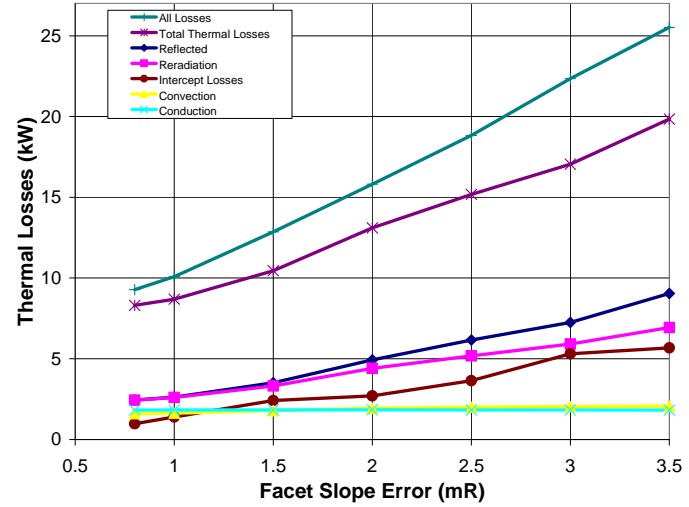


Figure 5. Thermal and intercept losses for different slope errors at the optimized aperture diameter.

simulation. This also emphasizes the need to evaluate slope error in terms of a “perfect shape” (parabola) instead of against the design shape, in cases where the design significantly differs from a parabola, such as the SAIC approach with flat subfacets.

In order to convert absorbed thermal energy into predicted net output power, we need to determine (by analysis) the absorbed power at various insolation levels, and then relate that to the measured system performance curve in Figure 1. I modeled the dish with 78 facets (4 facets removed) and determined the absorbed energy for the baseline system at 200 to 1000 W/m² insolation. The facets had been removed from the hardware system due to the high insolation levels available in Albuquerque, combined with several optical system improvements, in order to match the power input requirements of the engine. This is shown in Figure 6, along with the system performance curve from figure 1. At 200 W/m² insolation, the system net output power is 0, but the absorbed thermal power predicted is 10.7 kW. This represents the power that must be absorbed to overcome fixed thermal and mechanical losses within the engine. At 1000 W/m², the net system output power is 25 kW, with an absorbed thermal power of 68.9 kW. If we cross-plot these results, we find the system net output power vs. the absorbed power, as shown in Figure 7. The slope of this linear relationship indicates that 43% of additional absorbed power results in net electrical power out of the system, once the fixed losses are overcome. This curve is a fundamental characterization of the engine package based on measured electrical output data and modeled input thermal power. This can be applied to the full 82-facet system model.

COST/PERFORMANCE RELATIONSHIP

There are a number of ways to estimate the economic impact of facet performance. The simplest approach is to consider the value of the system at rated power based on the published baseline installed cost, at \$50,000 or \$2/W of rated power installed. The implicit assumption is that a complete economic analysis has been performed that indicates \$2/W is an appropriate cost to operate the systems and

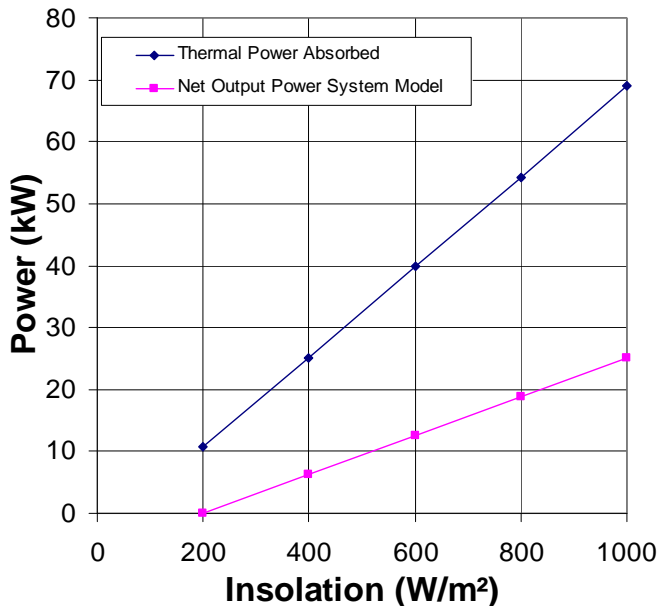


Figure 6. Thermal input and electrical net output for a 78-facet SES dish. The output is based on published data, while the input is based on the current work with CIRCE2 and AEETES models.

make a profit for the investors. If we calculate the difference in absorbed energy between the baseline case and any other case, from Figure 4, and then convert this difference in absorbed thermal power to a difference of rated output using Figure 7, we find the curves in Figure 8. The “optimum” aperture size was used for each slope error in Figure 8. If the system “value” is \$2/W installed based on the SES published goal cost and performance, then this reduction in system rated capacity is easily valued, also shown in Figure 8.

If we consider the case of 3.0 mrad slope error, compared to the

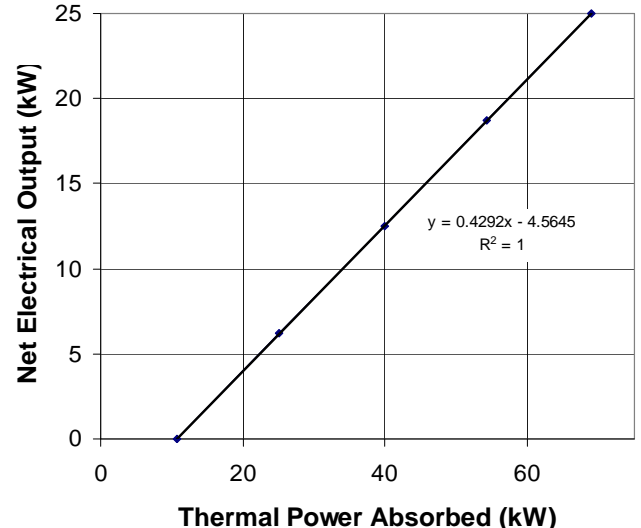


Figure 7. System performance curve for modeled input power to measured output electrical power. This cross-plot is used to evaluate the potential electrical output power for theoretical cases with reduced input absorbed power.

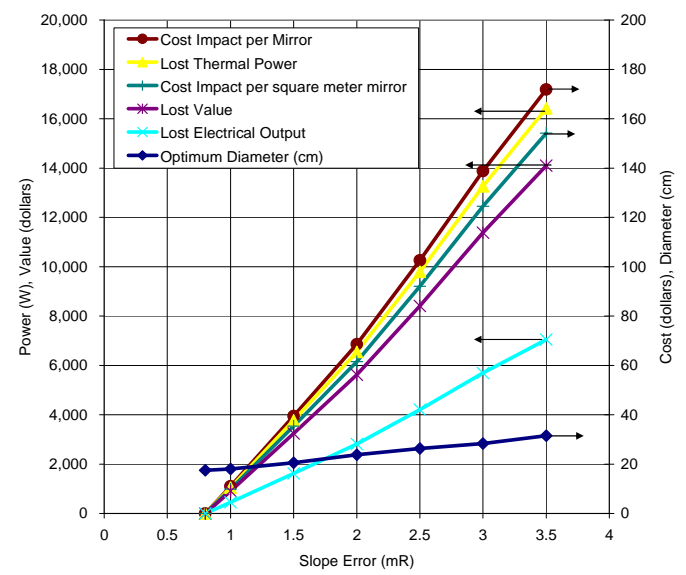


Figure 8. Losses due to slope error increases relative to the baseline case, and corresponding costs based on \$2/W installed system cost. For example, a 3.0 mrad facet would have to cost \$139 less than the baseline to have the same cost/performance ratio of \$2/W.

0.8 mrad baseline, we see the reduction in absorbed thermal power is over 13 kW (Lost Thermal Power in Figure 8), which reduces the rated output electrical energy by 5.7 kW (Lost Electrical Power). This reduction would mean the dish, which has not changed in size or complexity, would have to be installed for \$11.4k (Lost Value) less to break even at the \$2/W cost. Since nothing has changed except the facets, for 82 facets, the price for the facets would have to be reduced by \$139 each (Reduced Cost per Mirror) just to break even. This is more than the total estimated cost of the high performance prototype facets, even if the impact of inflation over the 1998 cost estimates is considered. Another way to look at this is if a \$30 facet is found at 3.0 mrad accuracy, one could afford to pay \$169 per 0.8 mrad facet and obtain the same cost/performance ratio. If the actual system installed cost is greater than \$2/W, then the cost of this reduction in performance is also increased proportionally.

A second approach to value the lost performance would be to add additional mirror area to compensate for the lost energy, so that the per-system rating remains 25 kW. However, this is a complex engineering problem. If we consider that 82 facets provide 60 kW thermal power to the absorber (3.0 mrad case), and we have to increase this by 13 kW, we would need roughly 18 more facets to provide this power. However, this substantially increases the size of the dish, which in turn increases the size of the aperture at the optimum, resulting in more thermal loss and requiring even more mirrors. We would not only have to consider the additional cost per facet, but also the cost of additional steel structure to support the new facets. In addition, the larger dishes would require a larger spacing in the field, with a cost in land, wiring, and maintenance time. It is likely these costs would far exceed the \$11.4k estimated in the simple analysis above.

A third method is to evaluate the change in annual energy production of the system with the change in mirror performance. One must develop a complete system performance curve, not just the rated performance at specification conditions. I ran the 0.8 and 3.0 mrad slope error mirror cases at insolation levels of 200 to 1000 W/m² with

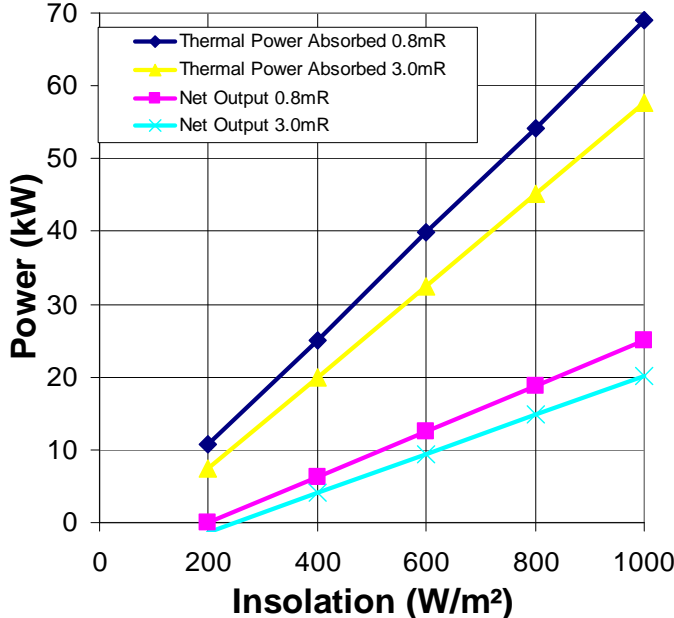


Figure 9. System models for 0.8 mrad and 3.0 mrad dish systems. Note the reduced performance across the entire operating range. These were both performed with 78 facets to remain compatible with the measured system data.

the CIRCE2 and AEETES models to generate the absorbed thermal power curve shown in Figure 9. I used the 78-facet model to remain compatible with the system model developed based on measured system data. Comparing this again as in Figure 7, we can generate a new system performance curve (net output power is derived from net absorbed power), also in Figure 9. The reduced performance results in a system net output model with 20 kW at 1000 W/m² insolation, and a zero intercept at 250 W/m² insolation. The baseline and 3.0 mrad system performance curves can be used in an annual performance model [29] to estimate the total system electrical energy delivered in a “typical” year. The model [29] uses Solergy [30] 15-minute weather data from 1977 at the Barstow Solar 1 location as a sample year, and calculates the energy produced every 15 minutes. I assumed the dishes have 100% availability and remain clean throughout the year. The model accounts for dish-to-dish shading and the impact this has on power production. Each baseline 78-mirror system produces 56.3 MW-hr in the modeled typical year, while the 3 mrad 78-mirror system only produces 44.0 MW-hr, for a net loss in energy produced of 12.3 MW-hr or 22%. These results are for an average dish in a 20,000-unit field of dishes. If we assume the energy is worth a nominal \$0.10/(kW-hr), with summer afternoon value at \$0.30/(kW-hr) and winter at \$0.06/(kW-hr), then the loss in revenue is \$1573/year for each system or \$31.5M/year for the field of 20,000 systems. The levelized energy cost can be expressed as:

$$LEC = \frac{FCR * CC + OM}{AE} \quad (1)$$

Where:

FCR=Fixed Charge Rate

CC=Capital Cost

OM=annual O&M cost

AE=annual energy production

If we re-arrange this, solving for capital cost, and take the derivative, we find:

$$\Delta CC = \frac{LEC * \Delta AE}{FCR} \quad (2)$$

The LEC*ΔAE term is the change in the annual cost of all the electricity generated. Instead of cost, we can replace this term with the change in *value* of the energy produced, then the result is the impact on the capital *value* rather than cost. If we use a FCR of 7.42% (based on an Investment Tax Credit (ITC) of 10%, 5 year accelerated depreciation, 50/50 debt-equity ratio, and no property tax) [31], and the change in the annual value of energy produced as \$1573, we find the change in the *value* of the capital equipment is over \$21,000.

SUMMARY/CONCLUSIONS

The use of the sandwich construction structural facets, at 0.8 mrad slope error, has raised the possibility of dramatically improving the performance of “commercial” dish systems. We have seen many attempts at commercial-cost facets have resulted in local slope errors in the 2-4 mrad range. In this paper, we used a case study of the SES/MDAC dish design with these high performance mirrors to examine the performance and economic impacts of a range of facet performance levels.

The poorer-quality facets impact performance primarily through loss-control aperture size, which increases dramatically with facet slope error. A point comparison of a 3.0 mrad facet design to the

current 0.8 mrad facet design indicates a 22.8% loss in peak performance, and a corresponding 21.8% loss in annual performance. This results in an estimated loss in value of the system of \$11k to \$21k, depending on the method used. Thus, one could pay \$139-\$256 more per facet for the higher quality facet and break even on price to value ratio. Similar details can be developed at any proposed slope error facet to determine the change in value of such a system compared to the baseline 0.8 mrad facet system.

The high temperature, high concentration nature of the dish-Stirling system makes the losses very closely coupled to aperture size. When other imperfections in the system are reasonably controlled, the aperture size is directly dependent upon the random local slope error of the facets. The final result is that the value of the system is strongly influenced by the accuracy of the facets incorporated, and the designer can afford to pay a substantial premium for high quality facets, assuming a path to automated production can be identified. Of the facets reviewed, the sandwich construction facets currently in use by SES remain a strong candidate. While reported slope errors vary, the stamped steel construction facets show promise. The slumped glass facets, currently popular for trough systems, also show the possibility of reaching acceptable performance, but have to be demonstrated in a dish system.

The application of this methodology to the SES system demonstrates the impact of reduced facet optical performance on system value. This same methodology can be applied, with similar results, to other dish systems with high temperature absorbers, such as dish-Brayton and thermochemical processes. The higher temperatures normally associated with these other cycles will increase the impact of thermal re-radiation losses. The additional losses were nearly equally split between thermal re-radiation, visible reflection, and increased intercept losses. Therefore, while the impact may be reduced somewhat, these conclusions also will apply to lower temperature systems, where reflection and intercept losses will still occur.

Similarly, the approach presented here can be applied to other point-focus systems (towers) and even line-focus systems. While some such systems (troughs) may not have a cavity to control re-radiation, loss mechanisms will still be driven by the receiver exposed area. An improved optical system can lead to higher net concentration ratios, with a corresponding improvement in system performance.

As Concentrating systems move from prototype to production, cost reduction is a driving factor. The approaches presented in this paper provide a framework in which performance reductions associated with cost reductions can be evaluated. For the studied system, it is apparent that there is considerable value in high performance optics. Therefore, cost reduction cannot be considered independent of performance impacts.

ACKNOWLEDGEMENTS

While this effort was based primarily on published data and exercising of Sandia National Laboratories software codes, the author would like to acknowledge the close cooperation with the SES team. Sandia is a multiprogram laboratory operated by Sandia Corporation, a Lockheed Martin Company, for the United States Department of Energy's National Nuclear Security Administration under contract DE-AC04-94AL85000.

REFERENCES

- [1] Andraka, C. E. and Powell, M. P., 2008, "Dish Stirling Development For Utility-Scale Commercialization," 14th Biennial CSP SolarPACES Symposium, Las Vegas, NV.
- [2] Liden, R., 2007, "Solar Dish Stirling Systems Report," NREL CSP Technology Workshop, Denver, CO.
- [3] Department of Energy 2004, "Solar Energy Technologies Program Multi-Year Technical Plan 2003-2007 and beyond," DOE/GO-102004-1775, U.S. Department of Energy, Energy Efficiency and Renewable Energy, Washington, DC.
- [4] Schmit, J., 2008, "Taking on the Solar Challenge," USA Today, 1-21-08.
- [5] Diver, R. B., and Andraka, C. E., 2003, "Integration of the Advanced Dish Development System," SAND2003-0780C, International Solar Energy Conference Proceedings, Kohala Coast, Hawaii Island, HI.
- [6] Diver, R. B., Andraka, C. E., Rawlinson, K. S., Moss, T. A., Goldberg, V., and Thomas, G., 2003, "Status of the Advanced Dish Development System Project," International Solar Energy Conference Proceedings, Kohala Coast, Hawaii Island, HI.
- [7] Diver, R. B., 1992, "Reflux Solar Receiver Design Considerations," Solar Engineering 1992, W. Stine, J. Kreider, and K. Watanabe, eds., American Society of Mechanical Engineers, New York, NY, **2**, pp. 981-989.
- [8] Jones, S. A., Gruetzner, J. K., Houser, R. M., Edgar, R. M., and Wendelin, T. J., 1997, "VSHOT Measurement Uncertainty and Experimental Sensitivity Study," IECEC-97: Proceedings of the Thirty-Second Intersociety Energy Conversion Engineering Conference, Honolulu, HI. Energy Systems, Renewable Energy Resources, Environmental Impact and Policy Impacts on Energy, American Institute of Chemical Engineers, New York, NY, **3**, pp. 1877-1882.
- [9] Diver R. B., Jones S. A., Robb S., and Mahoney A. R., 1995, "The Lustering of TBC-2," SAND94-1382, Sandia National Laboratories, Albuquerque, NM.
- [10] Washom, B., 1984, "Vanguard I Solar Parabolic Dish-Stirling Engine Module Final Report," DOE-AL-16333-2, Advanco Corporation and US Department of Energy, Albuquerque, NM.
- [11] Diver, R. B. and Stine, W. B., 1993, "A Compendium of Solar Dish/Stirling Technology," SAND93-7026, Sandia National Laboratories, Albuquerque, NM.
- [12] Wendelin, T. J. and Grossman, J. W., 1995, "Co-Validation of Three Methods for Optical Characterization of Point-Focus Concentrators," Proceedings of International Solar Energy Conference, Maui, HI.
- [13] Davenport, R. L., and Featherby, M., 2003, "Demonstration of a Novel Mirror Facet for Solar Concentrators," Proceedings of the 32nd ASES Annual Conference, Austin, TX.
- [14] Jones, S. A., 1999, "VSHOT Measurements of DISTAL II Dish Concentrators," SAND98-2778C, Proceedings of the Renewable and Advanced Energy Systems for the 21st Century, a joint ASME/JSME/JSES/KSME International Conference, Maui, HI.

[15] Lopez, C. W. and Stone, K. W., 1993, "Performance of the Southern California Edison Company Stirling Dish," SAND93-7098, Sandia National Laboratories, Albuquerque, NM.

[16] Lopez, C. W. and Stone, K. W., 1992, "Design and Performance of the Southern California Edison Stirling Dish," ASME J. of Solar Energy, **2**, pp. 945-952.

[17] Wendelin, T., May, K., and Gee, R., 2006, "Video Scanning Hartmann Optical Testing of State-of-the-Art Parabolic Trough Concentrators," Proceedings of Solar 2006 (ISEC 2006), Denver CO.

[18] Wendelin, T, 2008, Private email report of MDAC stampback facet measurement.

[19] Stone, K. W., Radtke, C. W., and Blackmon, J. B, 1993, "Status of Glass Reflector Technology for Heliostats and Concentrators," Proceedings of the 28th Intersociety Energy Conversion Engineering Conference, Atlanta, GA.

[20] Diver, R. B., and Grossman, J. W., 1999, "Sandwich Construction Solar Structural Facets," ASME International Solar Energy Conference, Maui, HI.

[21] Diver, R. B., Andraka, C. E., Rawlinson, K. S., Goldberg, V., and Thomas, G., 2001, "The Advanced Dish Development System Project," ASME Proceedings of Solar Forum 2001, Washington, D.C.

[22] Andraka, C. E., and Liden, R. L., 2006, "Stirling Energy Systems Model Power Plant: Bridge to Deployment," Solar Power 2006, SEPA, San Diego, CA.

[23] Andraka, C. E., 2007, "Alignment Strategy Optimization Method For Dish Stirling Faceted Concentrators," ES2007-36177, Proceedings of ES2007, ASME, Energy Sustainability 2007, Long Beach, CA.

[24] Andraka, C.E., 2007, "Dish Stirling Development," DOE program review and symposium, Denver, CO.

[25] Stine, W. B., 1995, "Experimentally Validated Long-Term Energy Production Prediction Model for Solar Dish/Stirling Electric Generating Systems," Paper Number 95-166, Proceedings of the Intersociety Energy Conversion Engineering Conference, D.Y. Goswami, L.D. Kannberg, T.R. Mancini, and S. Somasundaram, eds., American Society of Mechanical Engineers, New York, NY, **2**, pp. 491-495.

[26] Romero V. J., 1991, "CIRCE2/DEKGEN2: A Software Package for Facilitated Optical Analysis of 3-D Distributed Solar Energy Concentrators – Theory and User Manual," SAND91-2238, Sandia National Laboratories, Albuquerque, NM.

[27] Hogan Jr., R. E., 1992, "AEETES, A Solar Reflux Receiver Thermal Performance Numerical Model," ASME International Solar Energy Conference, Maui, HI.

[28] Stine, W. B. and McDonald, C. G., 1989, "Cavity Receiver Convective Heat Loss," Proceedings of the International Solar Energy Society, Solar World Congree 1989, Kobe, Japan, pp. 1318-1322.

[29] Igo, J., and Andraka, C. E., 2007, "Solar Dish Field System Model For Spacing Optimization," ES2007-36154, Proceedings of ES2007, ASME, Energy Sustainability 2007, Long Beach, CA.

[30] Stoddard, M. C., Faas, S. E., Chaing, C. J., and Dirks, J. A, 1987, "SOLERGY – A Computer Code for Calculating the Annual Energy from Central Receiver Power Plants," SAND86-8060, Sandia National Laboratories, Albuquerque NM.

[31] Sargent & Lundy Consulting Group, 2003, "Assessment of Parabolic Trough and Power Tower Solar Technology Cost and Performance Forecasts," SL-5641, Chicago IL.